

Study of hadronic transitions between Υ states and observation of $\Upsilon(4S) \rightarrow \eta\Upsilon(1S)$ decay

B. Aubert,¹ M. Bona,¹ Y. Karyotakis,¹ J. P. Lees,¹ V. Poireau,¹ E. Prencipe,¹ X. Prudent,¹ V. Tisserand,¹ J. Garra Tico,² E. Grauges,² L. Lopez^{ab,3} A. Palano^{ab,3} M. Pappagallo^{ab,3} G. Eigen,⁴ B. Stugu,⁴ L. Sun,⁴ G. S. Abrams,⁵ M. Battaglia,⁵ D. N. Brown,⁵ R. N. Cahn,⁵ R. G. Jacobsen,⁵ L. T. Kerth,⁵ Yu. G. Kolomensky,⁵ G. Kukartsev,⁵ G. Lynch,⁵ I. L. Osipenkov,⁵ M. T. Ronan,^{5,*} K. Tackmann,⁵ T. Tanabe,⁵ C. M. Hawkes,⁶ N. Soni,⁶ A. T. Watson,⁶ H. Koch,⁷ T. Schroeder,⁷ D. Walker,⁸ D. J. Asgeirsson,⁹ B. G. Fulsom,⁹ C. Hearty,⁹ T. S. Mattison,⁹ J. A. McKenna,⁹ M. Barrett,¹⁰ A. Khan,¹⁰ L. Teodorescu,¹⁰ V. E. Blinov,¹¹ A. D. Bukin,¹¹ A. R. Buzykaev,¹¹ V. P. Druzhinin,¹¹ V. B. Golubev,¹¹ A. P. Onuchin,¹¹ S. I. Serednyakov,¹¹ Yu. I. Skovpen,¹¹ E. P. Solodov,¹¹ K. Yu. Todyshev,¹¹ M. Bondioli,¹² S. Curry,¹² I. Eschrich,¹² D. Kirkby,¹² A. J. Lankford,¹² P. Lund,¹² M. Mandelkern,¹² E. C. Martin,¹² D. P. Stoker,¹² S. Abachi,¹³ C. Buchanan,¹³ J. W. Gary,¹⁴ F. Liu,¹⁴ O. Long,¹⁴ B. C. Shen,^{14,*} G. M. Vitug,¹⁴ Z. Yasin,¹⁴ L. Zhang,¹⁴ V. Sharma,¹⁵ C. Campagnari,¹⁶ T. M. Hong,¹⁶ D. Kovalskiy,¹⁶ M. A. Mazur,¹⁶ J. D. Richman,¹⁶ T. W. Beck,¹⁷ A. M. Eisner,¹⁷ C. J. Flacco,¹⁷ C. A. Heusch,¹⁷ J. Kroseberg,¹⁷ W. S. Lockman,¹⁷ T. Schalk,¹⁷ B. A. Schumm,¹⁷ A. Seiden,¹⁷ L. Wang,¹⁷ M. G. Wilson,¹⁷ L. O. Winstrom,¹⁷ C. H. Cheng,¹⁸ D. A. Doll,¹⁸ B. Echenard,¹⁸ F. Fang,¹⁸ D. G. Hitlin,¹⁸ I. Narsky,¹⁸ T. Piatenko,¹⁸ F. C. Porter,¹⁸ R. Andreassen,¹⁹ G. Mancinelli,¹⁹ B. T. Meadows,¹⁹ K. Mishra,¹⁹ M. D. Sokoloff,¹⁹ P. C. Bloom,²⁰ W. T. Ford,²⁰ A. Gaz,²⁰ J. F. Hirschauer,²⁰ A. Kreisel,²⁰ M. Nagel,²⁰ U. Nauenberg,²⁰ J. G. Smith,²⁰ K. A. Ulmer,²⁰ S. R. Wagner,²⁰ R. Ayad,^{21,†} A. Soffer,^{21,‡} W. H. Toki,²¹ R. J. Wilson,²¹ D. D. Altenburg,²² E. Feltresi,²² A. Hauke,²² H. Jasper,²² M. Karbach,²² J. Merkel,²² A. Petzold,²² B. Spaan,²² K. Wacker,²² M. J. Kobel,²³ W. F. Mader,²³ R. Nogowski,²³ K. R. Schubert,²³ R. Schwierz,²³ J. E. Sundermann,²³ A. Volk,²³ D. Bernard,²⁴ G. R. Bonneaud,²⁴ E. Latour,²⁴ Ch. Thiebaut,²⁴ M. Verderi,²⁴ P. J. Clark,²⁵ W. Gradl,²⁵ S. Playfer,²⁵ J. E. Watson,²⁵ M. Andreotti^{ab,26} D. Bettoni^{a,26} C. Bozzi^{a,26} R. Calabrese^{ab,26} A. Cecchi^{ab,26} G. Cibinetto^{ab,26} P. Franchini^{ab,26} E. Luppi^{ab,26} M. Negrini^{ab,26} A. Petrella^{ab,26} L. Piemontese^{a,26} V. Santoro^{ab,26} R. Baldini-Ferrolì,²⁷ A. Calcaterra,²⁷ R. de Sangro,²⁷ G. Finocchiaro,²⁷ S. Pacetti,²⁷ P. Patteri,²⁷ I. M. Peruzzi,^{27,§} M. Piccolo,²⁷ M. Rama,²⁷ A. Zallo,²⁷ A. Buzzo^{a,28} R. Contri^{ab,28} M. Lo Vetere^{ab,28} M. M. Macri^{a,28} M. R. Monge^{ab,28} S. Passaggio^{a,28} C. Patrignani^{ab,28} E. Robutti^{a,28} A. Santroni^{ab,28} S. Tosi^{ab,28} K. S. Chaisanguanthum,²⁹ M. Morii,²⁹ J. Marks,³⁰ S. Schenk,³⁰ U. Uwer,³⁰ V. Klose,³¹ H. M. Lacker,³¹ D. J. Bard,³² P. D. Dauncey,³² J. A. Nash,³² W. Panduro Vazquez,³² M. Tibbetts,³² P. K. Behera,³³ X. Chai,³³ M. J. Charles,³³ U. Mallik,³³ J. Cochran,³⁴ H. B. Crawley,³⁴ L. Dong,³⁴ W. T. Meyer,³⁴ S. Prell,³⁴ E. I. Rosenberg,³⁴ A. E. Rubin,³⁴ Y. Y. Gao,³⁵ A. V. Gritsan,³⁵ Z. J. Guo,³⁵ C. K. Lae,³⁵ A. G. Denig,³⁶ M. Fritsch,³⁶ G. Schott,³⁶ N. Arnaud,³⁷ J. Béquilleux,³⁷ A. D’Orazio,³⁷ M. Davier,³⁷ J. Firmino da Costa,³⁷ G. Grosdidier,³⁷ A. Höcker,³⁷ V. Lepeltier,³⁷ F. Le Diberder,³⁷ A. M. Lutz,³⁷ S. Pruvot,³⁷ P. Roudeau,³⁷ M. H. Schune,³⁷ J. Serrano,³⁷ V. Sordini,^{37,¶} A. Stocchi,³⁷ G. Wormser,³⁷ D. J. Lange,³⁸ D. M. Wright,³⁸ I. Bingham,³⁹ J. P. Burke,³⁹ C. A. Chavez,³⁹ J. R. Fry,³⁹ E. Gabathuler,³⁹ R. Gamet,³⁹ D. E. Hutchcroft,³⁹ D. J. Payne,³⁹ C. Touramanis,³⁹ A. J. Bevan,⁴⁰ C. K. Clarke,⁴⁰ K. A. George,⁴⁰ F. Di Lodovico,⁴⁰ R. Sacco,⁴⁰ M. Sigamani,⁴⁰ G. Cowan,⁴¹ H. U. Flaecher,⁴¹ D. A. Hopkins,⁴¹ S. Paramesvaran,⁴¹ F. Salvatore,⁴¹ A. C. Wren,⁴¹ D. N. Brown,⁴² C. L. Davis,⁴² K. E. Alwyn,⁴³ D. S. Bailey,⁴³ R. J. Barlow,⁴³ Y. M. Chia,⁴³ C. L. Edgar,⁴³ G. D. Lafferty,⁴³ T. J. West,⁴³ J. I. Yi,⁴³ J. Anderson,⁴⁴ C. Chen,⁴⁴ A. Jawahery,⁴⁴ D. A. Roberts,⁴⁴ G. Simi,⁴⁴ J. M. Tuggle,⁴⁴ C. Dallapiccola,⁴⁵ X. Li,⁴⁵ E. Salvati,⁴⁵ S. Saremi,⁴⁵ R. Cowan,⁴⁶ D. Dujmic,⁴⁶ P. H. Fisher,⁴⁶ K. Koeneke,⁴⁶ G. Sciolla,⁴⁶ M. Spitznagel,⁴⁶ F. Taylor,⁴⁶ R. K. Yamamoto,⁴⁶ M. Zhao,⁴⁶ P. M. Patel,⁴⁷ S. H. Robertson,⁴⁷ A. Lazzaro^{ab,48} V. Lombardo^{a,48} F. Palombo^{ab,48} J. M. Bauer,⁴⁹ L. Cremaldi,⁴⁹ V. Eschenburg,⁴⁹ R. Godang,^{49,**} R. Kroeger,⁴⁹ D. A. Sanders,⁴⁹ D. J. Summers,⁴⁹ H. W. Zhao,⁴⁹ M. Simard,⁵⁰ P. Taras,⁵⁰ F. B. Viaud,⁵⁰ H. Nicholson,⁵¹ G. De Nardo^{ab,52} L. Lista^{a,52} D. Monorchio^{ab,52} G. Onorato^{ab,52} C. Sciacca^{ab,52} G. Raven,⁵³ H. L. Snoek,⁵³ C. P. Jessop,⁵⁴ K. J. Knoepfel,⁵⁴ J. M. LoSecco,⁵⁴ W. F. Wang,⁵⁴ G. Benelli,⁵⁵ L. A. Corwin,⁵⁵ K. Honscheid,⁵⁵ H. Kagan,⁵⁵ R. Kass,⁵⁵ J. P. Morris,⁵⁵ A. M. Rahimi,⁵⁵ J. J. Regensburger,⁵⁵ S. J. Sekula,⁵⁵ Q. K. Wong,⁵⁵ N. L. Blount,⁵⁶ J. Brau,⁵⁶ R. Frey,⁵⁶ O. Igonkina,⁵⁶ J. A. Kolb,⁵⁶ M. Lu,⁵⁶ R. Rahmat,⁵⁶ N. B. Sinev,⁵⁶ D. Strom,⁵⁶ J. Strube,⁵⁶ E. Torrence,⁵⁶ G. Castelli^{ab,57} N. Gagliardi^{ab,57} M. Margoni^{ab,57} M. Morandin^{a,57} M. Posocco^{a,57} M. Rotondo^{a,57} F. Simonetto^{ab,57} R. Stroili^{ab,57} C. Voci^{ab,57} P. del Amo Sanchez,⁵⁸ E. Ben-Haim,⁵⁸ H. Briand,⁵⁸ G. Calderini,⁵⁸ J. Chauveau,⁵⁸ P. David,⁵⁸

Published in the Physical Review D

Work supported in part by US Department of Energy contract DE-AC02-76SF00515

L. Del Buono,⁵⁸ O. Hamon,⁵⁸ Ph. Leruste,⁵⁸ J. Ocariz,⁵⁸ A. Perez,⁵⁸ J. Prendki,⁵⁸ L. Gladney,⁵⁹ M. Biasini^{ab,60}
 R. Covarelli^{ab,60} E. Manoni^{ab,60} C. Angelini^{ab,61} G. Batignani^{ab,61} S. Bettarini^{ab,61} M. Carpinelli^{ab,61,††}
 A. Cervelli^{ab,61} F. Forti^{ab,61} M. A. Giorgi^{ab,61} A. Lusiani^{ac,61} G. Marchiori^{ab,61} M. Morganti^{ab,61} N. Neri^{ab,61}
 E. Paoloni^{ab,61} G. Rizzo^{ab,61} J. J. Walsh^{a,61} J. Biesiada,⁶² D. Lopes Pegna,⁶² C. Lu,⁶² J. Olsen,⁶² A. J. S. Smith,⁶²
 A. V. Telnov,⁶² F. Anulli^{a,63} E. Baracchini^{ab,63} G. Cavoto^{a,63} D. del Re^{ab,63} E. Di Marco^{ab,63} R. Faccini^{ab,63}
 F. Ferrarotto^{a,63} F. Ferroni^{ab,63} M. Gaspero^{ab,63} P. D. Jackson^{a,63} L. Li Gioi^{a,63} M. A. Mazzoni^{a,63} S. Morganti^{a,63}
 G. Piredda^{a,63} F. Polci^{ab,63} F. Renga^{ab,63} C. Voena^{a,63} M. Ebert,⁶⁴ T. Hartmann,⁶⁴ H. Schröder,⁶⁴ R. Waldi,⁶⁴
 T. Adye,⁶⁵ B. Franek,⁶⁵ E. O. Olaiya,⁶⁵ W. Roethel,⁶⁵ F. F. Wilson,⁶⁵ S. Emery,⁶⁶ M. Escalier,⁶⁶ L. Esteve,⁶⁶
 A. Gaidot,⁶⁶ S. F. Ganzhur,⁶⁶ G. Hamel de Monchenault,⁶⁶ W. Kozanecki,⁶⁶ G. Vasseur,⁶⁶ Ch. Yèche,⁶⁶
 M. Zito,⁶⁶ X. R. Chen,⁶⁷ H. Liu,⁶⁷ W. Park,⁶⁷ M. V. Purohit,⁶⁷ R. M. White,⁶⁷ J. R. Wilson,⁶⁷ M. T. Allen,⁶⁸
 D. Aston,⁶⁸ R. Bartoldus,⁶⁸ P. Bechtle,⁶⁸ J. F. Benitez,⁶⁸ R. Cenci,⁶⁸ J. P. Coleman,⁶⁸ M. R. Convery,⁶⁸
 J. C. Dingfelder,⁶⁸ J. Dorfan,⁶⁸ G. P. Dubois-Felsmann,⁶⁸ W. Dunwoodie,⁶⁸ R. C. Field,⁶⁸ A. M. Gabareen,⁶⁸
 S. J. Gowdy,⁶⁸ M. T. Graham,⁶⁸ P. Grenier,⁶⁸ C. Hast,⁶⁸ W. R. Innes,⁶⁸ J. Kaminski,⁶⁸ M. H. Kelsey,⁶⁸ H. Kim,⁶⁸
 P. Kim,⁶⁸ M. L. Kocian,⁶⁸ D. W. G. S. Leith,⁶⁸ S. Li,⁶⁸ B. Lindquist,⁶⁸ S. Luitz,⁶⁸ V. Luth,⁶⁸ H. L. Lynch,⁶⁸
 D. B. MacFarlane,⁶⁸ H. Marsiske,⁶⁸ R. Messner,⁶⁸ D. R. Muller,⁶⁸ H. Neal,⁶⁸ S. Nelson,⁶⁸ C. P. O'Grady,⁶⁸ I. Ofte,⁶⁸
 A. Perazzo,⁶⁸ M. Perl,⁶⁸ B. N. Ratcliff,⁶⁸ A. Roodman,⁶⁸ A. A. Salnikov,⁶⁸ R. H. Schindler,⁶⁸ J. Schwiening,⁶⁸
 A. Snyder,⁶⁸ D. Su,⁶⁸ M. K. Sullivan,⁶⁸ K. Suzuki,⁶⁸ S. K. Swain,⁶⁸ J. M. Thompson,⁶⁸ J. Va'vra,⁶⁸ A. P. Wagner,⁶⁸
 M. Weaver,⁶⁸ C. A. West,⁶⁸ W. J. Wisniewski,⁶⁸ M. Wittgen,⁶⁸ D. H. Wright,⁶⁸ H. W. Wulsin,⁶⁸ A. K. Yarritu,⁶⁸
 K. Yi,⁶⁸ C. C. Young,⁶⁸ V. Ziegler,⁶⁸ P. R. Burchat,⁶⁹ A. J. Edwards,⁶⁹ S. A. Majewski,⁶⁹ T. S. Miyashita,⁶⁹
 B. A. Petersen,⁶⁹ L. Wilden,⁶⁹ S. Ahmed,⁷⁰ M. S. Alam,⁷⁰ J. A. Ernst,⁷⁰ B. Pan,⁷⁰ M. A. Saeed,⁷⁰ S. B. Zain,⁷⁰
 S. M. Spanier,⁷¹ B. J. Wogslund,⁷¹ R. Eckmann,⁷² J. L. Ritchie,⁷² A. M. Ruland,⁷² C. J. Schilling,⁷²
 R. F. Schwitters,⁷² B. W. Drummond,⁷³ J. M. Izen,⁷³ X. C. Lou,⁷³ F. Bianchi^{ab,74} D. Gamba^{ab,74} M. Pelliccioni^{ab,74}
 M. Bomben^{ab,75} L. Bosisio^{ab,75} C. Cartaro^{ab,75} G. Della Ricca^{ab,75} L. Lanceri^{ab,75} L. Vitale^{ab,75} V. Azzolini,⁷⁶
 N. Lopez-March,⁷⁶ F. Martinez-Vidal,⁷⁶ D. A. Milanes,⁷⁶ A. Oyangueren,⁷⁶ J. Albert,⁷⁷ Sw. Banerjee,⁷⁷
 B. Bhuyan,⁷⁷ H. H. F. Choi,⁷⁷ K. Hamano,⁷⁷ R. Kowalewski,⁷⁷ M. J. Lewczuk,⁷⁷ I. M. Nugent,⁷⁷ J. M. Roney,⁷⁷
 R. J. Sobie,⁷⁷ T. J. Gershon,⁷⁸ P. F. Harrison,⁷⁸ J. Ilic,⁷⁸ T. E. Latham,⁷⁸ G. B. Mohanty,⁷⁸ H. R. Band,⁷⁹
 X. Chen,⁷⁹ S. Dasu,⁷⁹ K. T. Flood,⁷⁹ Y. Pan,⁷⁹ M. Pierini,⁷⁹ R. Prepost,⁷⁹ C. O. Vuosalo,⁷⁹ and S. L. Wu⁷⁹

(The BABAR Collaboration)

¹Laboratoire de Physique des Particules, IN2P3/CNRS et Université de Savoie, F-74941 Annecy-Le-Vieux, France

²Universitat de Barcelona, Facultat de Física, Departament ECM, E-08028 Barcelona, Spain

³INFN Sezione di Bari^a; Dipartimento di Fisica, Università di Bari^b, I-70126 Bari, Italy

⁴University of Bergen, Institute of Physics, N-5007 Bergen, Norway

⁵Lawrence Berkeley National Laboratory and University of California, Berkeley, California 94720, USA

⁶University of Birmingham, Birmingham, B15 2TT, United Kingdom

⁷Ruhr Universität Bochum, Institut für Experimentalphysik 1, D-44780 Bochum, Germany

⁸University of Bristol, Bristol BS8 1TL, United Kingdom

⁹University of British Columbia, Vancouver, British Columbia, Canada V6T 1Z1

¹⁰Brunel University, Uxbridge, Middlesex UB8 3PH, United Kingdom

¹¹Budker Institute of Nuclear Physics, Novosibirsk 630090, Russia

¹²University of California at Irvine, Irvine, California 92697, USA

¹³University of California at Los Angeles, Los Angeles, California 90024, USA

¹⁴University of California at Riverside, Riverside, California 92521, USA

¹⁵University of California at San Diego, La Jolla, California 92093, USA

¹⁶University of California at Santa Barbara, Santa Barbara, California 93106, USA

¹⁷University of California at Santa Cruz, Institute for Particle Physics, Santa Cruz, California 95064, USA

¹⁸California Institute of Technology, Pasadena, California 91125, USA

¹⁹University of Cincinnati, Cincinnati, Ohio 45221, USA

²⁰University of Colorado, Boulder, Colorado 80309, USA

²¹Colorado State University, Fort Collins, Colorado 80523, USA

²²Technische Universität Dortmund, Fakultät Physik, D-44221 Dortmund, Germany

²³Technische Universität Dresden, Institut für Kern- und Teilchenphysik, D-01062 Dresden, Germany

²⁴Laboratoire Leprince-Ringuet, CNRS/IN2P3, Ecole Polytechnique, F-91128 Palaiseau, France

²⁵University of Edinburgh, Edinburgh EH9 3JZ, United Kingdom

²⁶INFN Sezione di Ferrara^a; Dipartimento di Fisica, Università di Ferrara^b, I-44100 Ferrara, Italy

²⁷INFN Laboratori Nazionali di Frascati, I-00044 Frascati, Italy

²⁸INFN Sezione di Genova^a; Dipartimento di Fisica, Università di Genova^b, I-16146 Genova, Italy

²⁹Harvard University, Cambridge, Massachusetts 02138, USA

³⁰Universität Heidelberg, Physikalisches Institut, Philosophenweg 12, D-69120 Heidelberg, Germany

- ³¹Humboldt-Universität zu Berlin, Institut für Physik, Newtonstr. 15, D-12489 Berlin, Germany
- ³²Imperial College London, London, SW7 2AZ, United Kingdom
- ³³University of Iowa, Iowa City, Iowa 52242, USA
- ³⁴Iowa State University, Ames, Iowa 50011-3160, USA
- ³⁵Johns Hopkins University, Baltimore, Maryland 21218, USA
- ³⁶Universität Karlsruhe, Institut für Experimentelle Kernphysik, D-76021 Karlsruhe, Germany
- ³⁷Laboratoire de l'Accélérateur Linéaire, IN2P3/CNRS et Université Paris-Sud 11, Centre Scientifique d'Orsay, B. P. 34, F-91898 Orsay Cedex, France
- ³⁸Lawrence Livermore National Laboratory, Livermore, California 94550, USA
- ³⁹University of Liverpool, Liverpool L69 7ZE, United Kingdom
- ⁴⁰Queen Mary, University of London, London, E1 4NS, United Kingdom
- ⁴¹University of London, Royal Holloway and Bedford New College, Egham, Surrey TW20 0EX, United Kingdom
- ⁴²University of Louisville, Louisville, Kentucky 40292, USA
- ⁴³University of Manchester, Manchester M13 9PL, United Kingdom
- ⁴⁴University of Maryland, College Park, Maryland 20742, USA
- ⁴⁵University of Massachusetts, Amherst, Massachusetts 01003, USA
- ⁴⁶Massachusetts Institute of Technology, Laboratory for Nuclear Science, Cambridge, Massachusetts 02139, USA
- ⁴⁷McGill University, Montréal, Québec, Canada H3A 2T8
- ⁴⁸INFN Sezione di Milano^a; Dipartimento di Fisica, Università di Milano^b, I-20133 Milano, Italy
- ⁴⁹University of Mississippi, University, Mississippi 38677, USA
- ⁵⁰Université de Montréal, Physique des Particules, Montréal, Québec, Canada H3C 3J7
- ⁵¹Mount Holyoke College, South Hadley, Massachusetts 01075, USA
- ⁵²INFN Sezione di Napoli^a; Dipartimento di Scienze Fisiche, Università di Napoli Federico II^b, I-80126 Napoli, Italy
- ⁵³NIKHEF, National Institute for Nuclear Physics and High Energy Physics, NL-1009 DB Amsterdam, The Netherlands
- ⁵⁴University of Notre Dame, Notre Dame, Indiana 46556, USA
- ⁵⁵Ohio State University, Columbus, Ohio 43210, USA
- ⁵⁶University of Oregon, Eugene, Oregon 97403, USA
- ⁵⁷INFN Sezione di Padova^a; Dipartimento di Fisica, Università di Padova^b, I-35131 Padova, Italy
- ⁵⁸Laboratoire de Physique Nucléaire et de Hautes Energies, IN2P3/CNRS, Université Pierre et Marie Curie-Paris6, Université Denis Diderot-Paris7, F-75252 Paris, France
- ⁵⁹University of Pennsylvania, Philadelphia, Pennsylvania 19104, USA
- ⁶⁰INFN Sezione di Perugia^a; Dipartimento di Fisica, Università di Perugia^b, I-06100 Perugia, Italy
- ⁶¹INFN Sezione di Pisa^a; Dipartimento di Fisica, Università di Pisa^b; Scuola Normale Superiore di Pisa^c, I-56127 Pisa, Italy
- ⁶²Princeton University, Princeton, New Jersey 08544, USA
- ⁶³INFN Sezione di Roma^a; Dipartimento di Fisica, Università di Roma La Sapienza^b, I-00185 Roma, Italy
- ⁶⁴Universität Rostock, D-18051 Rostock, Germany
- ⁶⁵Rutherford Appleton Laboratory, Chilton, Didcot, Oxon, OX11 0QX, United Kingdom
- ⁶⁶DSM/Dapnia, CEA/Saclay, F-91191 Gif-sur-Yvette, France
- ⁶⁷University of South Carolina, Columbia, South Carolina 29208, USA
- ⁶⁸Stanford Linear Accelerator Center, Stanford, California 94309, USA
- ⁶⁹Stanford University, Stanford, California 94305-4060, USA
- ⁷⁰State University of New York, Albany, New York 12222, USA
- ⁷¹University of Tennessee, Knoxville, Tennessee 37996, USA
- ⁷²University of Texas at Austin, Austin, Texas 78712, USA
- ⁷³University of Texas at Dallas, Richardson, Texas 75083, USA
- ⁷⁴INFN Sezione di Torino^a; Dipartimento di Fisica Sperimentale, Università di Torino^b, I-10125 Torino, Italy
- ⁷⁵INFN Sezione di Trieste^a; Dipartimento di Fisica, Università di Trieste^b, I-34127 Trieste, Italy
- ⁷⁶IFIC, Universitat de Valencia-CSIC, E-46071 Valencia, Spain
- ⁷⁷University of Victoria, Victoria, British Columbia, Canada V8W 3P6
- ⁷⁸Department of Physics, University of Warwick, Coventry CV4 7AL, United Kingdom
- ⁷⁹University of Wisconsin, Madison, Wisconsin 53706, USA

We present a study of hadronic transitions between $\Upsilon(mS)$ ($m = 4, 3, 2$) and $\Upsilon(nS)$ ($n = 2, 1$) resonances based on 347.5 fb^{-1} of data taken with the BABAR detector at the PEP-II storage rings. We report the first observation of $\Upsilon(4S) \rightarrow \eta\Upsilon(1S)$ decay with a branching fraction $\mathcal{B}(\Upsilon(4S) \rightarrow \eta\Upsilon(1S)) = (1.96 \pm 0.06_{\text{stat}} \pm 0.09_{\text{syst}}) \times 10^{-4}$ and measure the ratio of partial widths $\Gamma(\Upsilon(4S) \rightarrow \eta\Upsilon(1S))/\Gamma(\Upsilon(4S) \rightarrow \pi^+\pi^-\Upsilon(1S)) = 2.41 \pm 0.40_{\text{stat}} \pm 0.12_{\text{syst}}$. We set 90% CL upper limits on the ratios $\Gamma(\Upsilon(2S) \rightarrow \eta\Upsilon(1S))/\Gamma(\Upsilon(2S) \rightarrow \pi^+\pi^-\Upsilon(1S)) < 5.2 \times 10^{-3}$ and $\Gamma(\Upsilon(3S) \rightarrow \eta\Upsilon(1S))/\Gamma(\Upsilon(3S) \rightarrow \pi^+\pi^-\Upsilon(1S)) < 1.9 \times 10^{-2}$. We also present new measurements

of the ratios $\Gamma(\Upsilon(4S) \rightarrow \pi^+\pi^-\Upsilon(2S))/\Gamma(\Upsilon(4S) \rightarrow \pi^+\pi^-\Upsilon(1S)) = 1.16 \pm 0.16_{stat} \pm 0.14_{syst}$ and $\Gamma(\Upsilon(3S) \rightarrow \pi^+\pi^-\Upsilon(2S))/\Gamma(\Upsilon(3S) \rightarrow \pi^+\pi^-\Upsilon(1S)) = 0.577 \pm 0.026_{stat} \pm 0.060_{syst}$.

PACS numbers: 14.40.Gx,13.25.Gv

I. INTRODUCTION

Hadronic transitions between bound states of heavy quarkonia [1] are generally studied using the QCD multipole expansion model (QCDME) [2]. This succeeds in explaining the relative rates of the $\psi(2S) \rightarrow \eta J/\psi$ and $\psi(2S) \rightarrow \pi\pi J/\psi$ transitions and the $\pi\pi$ invariant mass distributions in $\psi(2S) \rightarrow \pi\pi J/\psi$, $\Upsilon(2S) \rightarrow \pi\pi\Upsilon(1S)$, $\Upsilon(3S) \rightarrow \pi\pi\Upsilon(2S)$ and the recently observed $\Upsilon(4S) \rightarrow \pi^+\pi^-\Upsilon(1S)$ decays [3, 4]. Until recently the only feature that QCDME could not explain was the dipion invariant mass distribution in the $\Upsilon(3S) \rightarrow \pi\pi\Upsilon(1S)$ transition [5], for which a number of possible explanations have been proposed [6]. The dipion invariant mass distribution in $\Upsilon(4S) \rightarrow \pi^+\pi^-\Upsilon(2S)$ [3] is also in disagreement with the QCDME prediction and was not predicted either by the alternative explanations proposed for the $\Upsilon(3S) \rightarrow \pi^+\pi^-\Upsilon(1S)$. This implies that additional experimental input is needed to understand hadronic transitions. In QCDME the gluon radiation from a heavy $q\bar{q}$ bound state is calculated in terms of chromo-electric and chromo-magnetic fields, in analogy to electromagnetism. Transitions between colorless hadrons require the emission of at least two gluons. The $\Upsilon(mS) \rightarrow \pi\pi\Upsilon(nS)$ transitions ($m^3S_1 \rightarrow \pi\pi n^3S_1$ in spectroscopic notation [7]) are E1E1, i.e. transitions where both gluons are in an E1 state. The decays $\Upsilon(mS) \rightarrow \eta\Upsilon(nS)$ ($m^3S_1 \rightarrow \eta n^3S_1$) proceed either via E1M2 or M1M1 transitions; the E1M2 transition is expected to dominate. The $b\bar{b}$ system offers unique opportunities: there are five known $m^3S_1 \rightarrow \pi\pi n^3S_1$ transitions and also four kinematically allowed transitions involving an η meson. Of the latter only the $\Upsilon(2S) \rightarrow \eta\Upsilon(1S)$ has been recently observed by CLEO [8], with a branching fraction $\mathcal{B}(\Upsilon(2S) \rightarrow \eta\Upsilon(1S)) = (2.1_{-0.6}^{+0.7} \pm 0.5) \times 10^{-4}$.

In this paper we present improved measurements of the $\Upsilon(4S) \rightarrow \Upsilon(nS)$ transitions, a search for $\Upsilon(mS) \rightarrow \eta\Upsilon(1S)$ and new measurements of $\Upsilon(3S) \rightarrow \pi^+\pi^-\Upsilon(nS)$ and $\Upsilon(2S) \rightarrow \pi^+\pi^-\Upsilon(1S)$ partial widths. We also measure the ratios of partial widths $\Gamma(\Upsilon(mS) \rightarrow \eta\Upsilon(1S))/\Gamma(\Upsilon(mS) \rightarrow \pi^+\pi^-\Upsilon(1S))$ and $\Gamma(\Upsilon(mS) \rightarrow$

$\pi^+\pi^-\Upsilon(2S))/\Gamma(\Upsilon(mS) \rightarrow \pi^+\pi^-\Upsilon(1S))$ ($m = 3, 4$), for which a number of systematic uncertainties cancel.

The $\Upsilon(mS) \rightarrow \pi^+\pi^-\Upsilon(nS)$ and $\Upsilon(mS) \rightarrow \eta\Upsilon(nS)$ transitions, denoted by $mS \rightarrow \pi\pi nS$ and $mS \rightarrow \eta nS$, respectively, are studied by reconstructing the $\Upsilon(nS)$ mesons via their leptonic decay to $\mu^+\mu^-$ or e^+e^- . The η meson is reconstructed via its $\pi^+\pi^-\pi^0$ decay. With the choice of this particular η decay mode all final states contain the same charged particles, resulting in larger cancellations of the systematic uncertainties for the ratios of partial widths. Events where the η decays to $\gamma\gamma$ are not considered in this work because the $\ell\ell\gamma\gamma$ final state has a smaller signal to background ratio than the $\ell^+\ell^-\pi^+\pi^-\pi^0$ final state.

II. DATA SAMPLES AND DETECTOR

We search for $\Upsilon(4S)$ hadronic transitions using a sample of $(383.2 \pm 4.2) \times 10^6$ $\Upsilon(4S)$ decays corresponding to an integrated luminosity, L_{on}^{int} , of 347.5 fb^{-1} acquired near the peak of the $\Upsilon(4S)$ resonance (“on-peak”, nominal center-of-mass energy, \sqrt{s} of about 10.58 GeV) with the BABAR detector at the PEP-II asymmetric-energy e^+e^- storage rings at SLAC. In addition, a data sample corresponding to $L_{off}^{int} = 36.6 \text{ fb}^{-1}$, collected approximately 40 MeV below the resonance (“off-peak”) is used to study some of the backgrounds. Decays of $\Upsilon(3S)$ and $\Upsilon(2S)$ are studied in events recorded “on-peak” and selected with an initial state radiation (ISR) photon. The ISR photon, preferentially emitted at small angle along the beam direction, is not required to be detected.

The BABAR detector is described in detail elsewhere [9]. Charged-particle momenta are measured in a tracking system consisting of a five-layer double-sided silicon vertex tracker (SVT) and a 40-layer central drift chamber (DCH), both embedded in a 1.5-T axial magnetic field. Charged-particle identification is based on the specific energy loss measured in the SVT and DCH, and on a measurement of the photons produced in the fused-silica bars of the ring-imaging Cherenkov detector (DIRC). A CsI(Tl) electromagnetic calorimeter (EMC) is used to detect and identify photons and electrons, while muons are identified in the instrumented flux return of the magnet (IFR).

Simulated Monte Carlo (MC) events are generated using the EvtGen package [10]. The angular distribution of generated dilepton decays incorporates the $\Upsilon(nS)$ polarization, while dipion transitions are generated according to phase space. In the simulation of $mS \rightarrow \eta 1S$ we use the angular distribution dictated by the quantum numbers for a vector decay to a pseudoscalar and a vector. Secondary photon emission is taken into account

*Deceased

†Now at Temple University, Philadelphia, Pennsylvania 19122, USA

‡Now at Tel Aviv University, Tel Aviv, 69978, Israel

§Also with Università di Perugia, Dipartimento di Fisica, Perugia, Italy

¶Also with Università di Roma La Sapienza, I-00185 Roma, Italy

**Now at University of South Alabama, Mobile, Alabama 36688, USA

††Also with Università di Sassari, Sassari, Italy

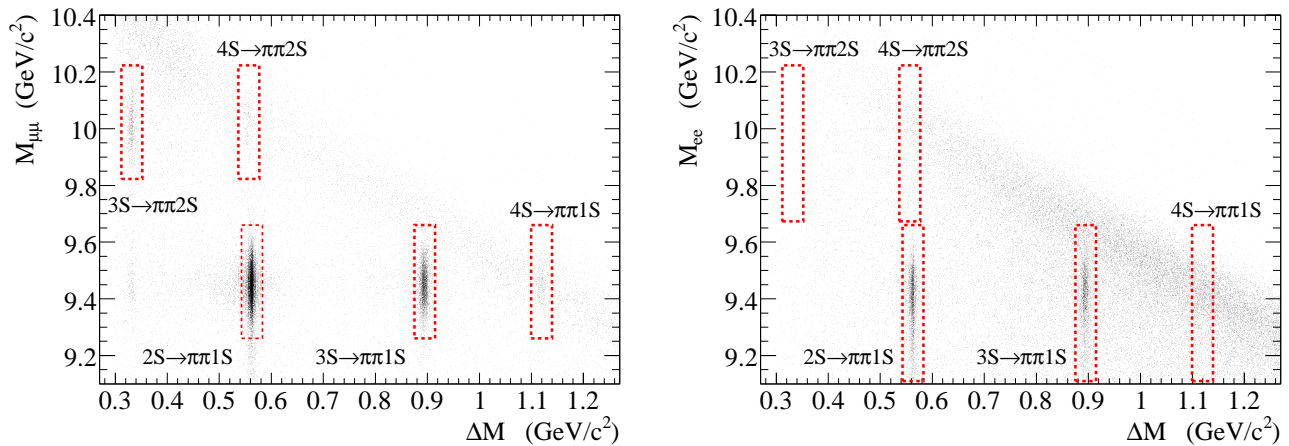


FIG. 1: $M_{\ell\ell}$ vs ΔM distributions of candidates after the preliminary selection for the $\mu\mu$ (left) and ee (right) samples. Dashed lines delimit the signal boxes for $mS \rightarrow \pi\pi nS$ transitions. The cluster of events in the lower left corner is due to $\Upsilon(3S) \rightarrow \pi^+\pi^-\Upsilon(2S)$ where the $\Upsilon(2S)$ subsequently decays to $\Upsilon(1S) X$.

in the simulation of $\Upsilon(mS)$ produced in ISR. Simulated events are passed through a detector simulation based on GEANT4 [11], and analyzed in the same manner as data.

III. EVENT SELECTION

The events of interest have a lepton pair from the decay of the $\Upsilon(nS)$ resonance of invariant mass, $M_{\ell\ell}$, compatible with the known mass values of the $\Upsilon(nS)$ [12], $M(nS)$, and a pair of oppositely charged pions.

The signature for $mS \rightarrow \pi\pi nS$ transition events is an invariant mass difference $\Delta M = M_{\pi\pi\ell\ell} - M_{\ell\ell}$ compatible with the difference of the masses of the two Υ resonances, $M(mS) - M(nS)$, where $M_{\pi\pi\ell\ell}$ is the $\pi^+\pi^-\ell^+\ell^-$ invariant mass.

The $mS \rightarrow \eta nS$ events have two additional photons from the π^0 decay, a $\pi^+\pi^-\pi^0$ invariant mass, $m_{3\pi}$, compatible with the known η mass, $M(\eta)$, and an invariant mass difference, $\Delta M_\eta = M_{3\pi\ell\ell} - M_{\ell\ell} - m_{3\pi}$ compatible with $M(mS) - M(nS) - M(\eta)$, where $M_{3\pi\ell\ell}$ is the $\pi^+\pi^-\pi^0\ell^+\ell^-$ invariant mass.

The r.m.s. widths of the reconstructed $M_{\ell\ell}$, $m_{3\pi}$, ΔM , and ΔM_η distributions are of the order of 75 MeV/c², 12 MeV/c², 7 MeV/c² and 10 MeV/c², respectively.

Events in the data sample with $M_{\ell\ell}$ within 350 MeV/c² of the known $M(nS)$ values and ΔM within 60 MeV/c² of the values expected for any of the $mS \rightarrow \pi\pi nS$ transitions were not examined until the event selection criteria were finalized. Events outside these regions were used to understand the background. Simulated MC events were used to model the signal.

Candidate events have at least 4 charged tracks with a polar angle θ within the fiducial volume of the tracking system ($0.41 < \theta < 2.54$ rad). Each lepton candidate is required to have a center-of-mass momentum be-

tween 4.20 GeV/c and 5.25 GeV/c. At least one of the muons of $\Upsilon(nS) \rightarrow \mu^+\mu^-$ candidates must be compatible with the muon hypothesis based on the energy deposited in the EMC and the hit pattern in the IFR along the track trajectory. Similarly at least one of the electrons of $\Upsilon(nS) \rightarrow e^+e^-$ candidates must be compatible with the electron hypothesis based on the energy deposit in the EMC, the ratio of energy in the EMC to the track momentum, and the energy loss in the detector material. We require $M_{\mu\mu}[M_{ee}]$ to be within ± 200 [-350,+200] MeV/c² of the nominal $\Upsilon(1S)$ or $\Upsilon(2S)$ mass. The asymmetric cut in the e^+e^- sample is due to bremsstrahlung, which causes a long tail in the reconstructed M_{ee} distribution at low invariant masses and that is partially recovered by an algorithm that combines the energy of electron tracks with the energy of nearby photons.

Pairs of oppositely charged tracks, not identified as electrons and whose Cherenkov angle in the DIRC, when measured, is within 3σ of the value expected for a pion, are selected to form a dipion candidate. The dilepton and the dipion are constrained to a common vertex and the vertex fit is required to have a χ^2 probability larger than 10^{-3} .

A large fraction of the remaining background is due to $e^+e^-\gamma$ and $\mu^+\mu^-\gamma$ events where a photon converts in the detector material and the leptons are reconstructed as pions. To reduce this background we reject events where the opening angle of the charged pion candidates in the laboratory reference frame has $\cos\theta_{\pi^+\pi^-} > 0.95$, or where the invariant mass of the charged tracks associated with the pion candidates, calculated assuming the e^\pm mass hypothesis, satisfies $m_{conv} < 50$ MeV/c². The distribution of $M_{\ell\ell}$ vs ΔM for candidate events after the preliminary selection is shown in Fig. 1.

In the case of $\Upsilon(4S) \rightarrow \Upsilon(nS)$ transitions the back-

TABLE I: Selection efficiencies for all studied transitions, separately for $\Upsilon(nS) \rightarrow \mu^+\mu^-$ and e^+e^- as determined by MC simulation. For the $mS \rightarrow \pi\pi nS$ transitions we quote both the efficiency averaged over phase space, ε_{PS} , and the effective efficiency, ε_{eff} , calculated according to Eq. 3.

Transition	Selection efficiency (%)			
	$\mu\mu$		ee	
	ε_{PS}	ε_{eff}	ε_{PS}	ε_{eff}
$2S \rightarrow \pi\pi 1S$	34.46±0.05	36.62±0.08	11.17±0.03	11.45±0.14
$3S \rightarrow \pi\pi 1S$	41.23±0.05	34.18±0.20	24.48±0.05	23.96±0.24
$3S \rightarrow \pi\pi 2S$	14.76±0.04	17.2 ±0.6	≈ 0	–
$4S \rightarrow \pi\pi 1S$	41.53±0.23	44.2 ±1.2	18.04±0.18	19.7 ±2.4
$4S \rightarrow \pi\pi 2S$	32.69±0.22	30.2 ±0.8	6.17±0.12	7.9 ±3.4
	ε		ε	
$2S \rightarrow \eta 1S$	8.25±0.09		≈ 0	
$3S \rightarrow \eta 1S$	9.42±0.10		3.91±0.06	
$4S \rightarrow \eta 1S$	10.07±0.10		3.77±0.06	

ground is larger and the expected signal smaller. For this reason we further restrict our selection to events where at least one of the two charged pions has a transverse momentum greater than 100 MeV/c, $m_{conv} > 100$ MeV/c², and the polar angle in the laboratory system of the e^- from $\Upsilon(nS) \rightarrow e^+e^-$ is larger than 0.7 rad, to reject radiative Bhabha events.

Events with at least two candidate photons of $E_\gamma > 50$ MeV and invariant mass $110 < m_{\gamma\gamma} < 150$ MeV/c² are considered to be ηnS candidates if the $\pi^+\pi^-\pi^0$ invariant mass is within 35 MeV/c² of the known η mass. To suppress possible cross-feed from the high statistics $mS \rightarrow \pi\pi nS$ transitions we require that $mS \rightarrow \eta nS$ candidates have ΔM more than 20 MeV/c² ($\approx 3\sigma$) from any of the known $M(mS) - M(nS)$ values.

We select $\Upsilon(2S)$ and $\Upsilon(3S)$ states produced via ISR, requiring that the momentum of the reconstructed $\ell^+\ell^-\pi^+\pi^-[\pi^0]$ in the center of mass rest frame, p_{cand}^* , is within ± 150 MeV/c of the expected value of $(s - M^2(mS)) / (2\sqrt{s})$. For $\Upsilon(4S)$ decays p_{cand}^* is required to be < 200 MeV/c.

The average efficiency for each of the transitions is given in Table I. The efficiency for the $\pi^+\pi^-[\pi^0]e^+e^-$ final state is in all cases smaller than for the $\pi^+\pi^-[\pi^0]\mu^+\mu^-$ final state due to a trigger-level inefficiency introduced by the prescaling of Bhabha scattering events, whose signature is given by two electrons of large invariant mass and no additional charged track of transverse momentum greater than 250 MeV/c. Because of the limited phase-space available in the $2S \rightarrow \eta 1S$ and $3S \rightarrow \pi\pi 2S$ decays, the momentum of the charged pions is always below the threshold, thus the efficiency for these two transitions is nearly zero when the $\Upsilon(nS)$ decays to e^+e^- .

IV. SIGNAL YIELDS

A. $\Upsilon(mS) \rightarrow \pi^+\pi^-\Upsilon(nS)$

The ΔM distributions of events in the final sample for the $mS \rightarrow \pi\pi nS$ transitions are shown in Fig. 2.

We determine the efficiency corrected signal yield for the $mS \rightarrow \pi\pi nS$ transitions without any assumption on the angular distributions of the decays. We divide the $2S \rightarrow \pi\pi 1S$ and $3S \rightarrow \pi\pi 1S$ samples into 10×6 bins of $m_{\pi\pi}$ and $\cos\theta_h$, where $m_{\pi\pi}$ is the $\pi^+\pi^-$ invariant mass and θ_h is the helicity angle of the π^+ , defined as the angle between the π^+ direction in the $\pi\pi$ rest frame and the $\pi\pi$ direction in the candidate $\Upsilon(mS)$ rest frame. The $3S \rightarrow \pi\pi 2S$ and $4S \rightarrow \pi\pi nS$ samples are divided into 6×4 bins of $m_{\pi\pi}$ and $\cos\theta_h$.

The signal yield in each bin is determined by a fit to the ΔM distribution, by maximizing the unbinned extended likelihood to the sum of a background probability density function (PDF) and a signal PDF. The signal PDF is parametrized by a Voigtian function (convolution of a Lorentzian with a Gaussian function), that is found to describe well the measured ΔM distribution for simulated events. The background is parametrized by a linear function. The resolution parameters for the signal PDF are fixed to the values determined by the simulation, thus the free parameters in the fits for bin i are: ΔM_{sig}^i , the peak position of the signal distribution, N_{sig}^i and N_{bkg}^i , the number of signal and background events, and the background shape parameters. The efficiency corrected signal yield for each $mS \rightarrow \pi\pi nS$ transition is then obtained as

$$N_{corr} = \sum_{i=1}^{nbins} N_{sig}^i / \varepsilon_i, \quad (1)$$

where $nbins$ is the number of bins (60 or 24) and ε_i is the efficiency in each bin determined from MC simulation.

B. $\Upsilon(mS) \rightarrow \eta\Upsilon(1S)$

Figure 3 shows the $m_{3\pi}$ vs ΔM_η distributions for events selected as $mS \rightarrow \eta 1S$ candidates. The widths of the signal boxes have been chosen as $\approx \pm 3\sigma$ in both variables based on MC simulation: $|m_{3\pi} - m_\eta| < 35$ MeV/c² and $|M(mS) - M(1S) - M(\eta) - \Delta M_\eta| < 30$ MeV/c². For the $2S \rightarrow \eta 1S$ transition we require $\Delta M_\eta < 30$ MeV/c² because the signal for this transition is expected close to the kinematic limit.

The numbers of candidates in the $2S \rightarrow \eta 1S$ and $3S \rightarrow \eta 1S$ signal boxes, shown in Table II, are compatible with the backgrounds extrapolated from the sidebands defined in Fig. 3. Thus, we have no signal for the $2S \rightarrow \eta 1S$ and $3S \rightarrow \eta 1S$ transitions.

We observe 56 candidates for the $4S \rightarrow \eta 1S$ transition in the “on-peak” data sample, and no candidates in the “off-peak” data sample. We test the hypothesis that the

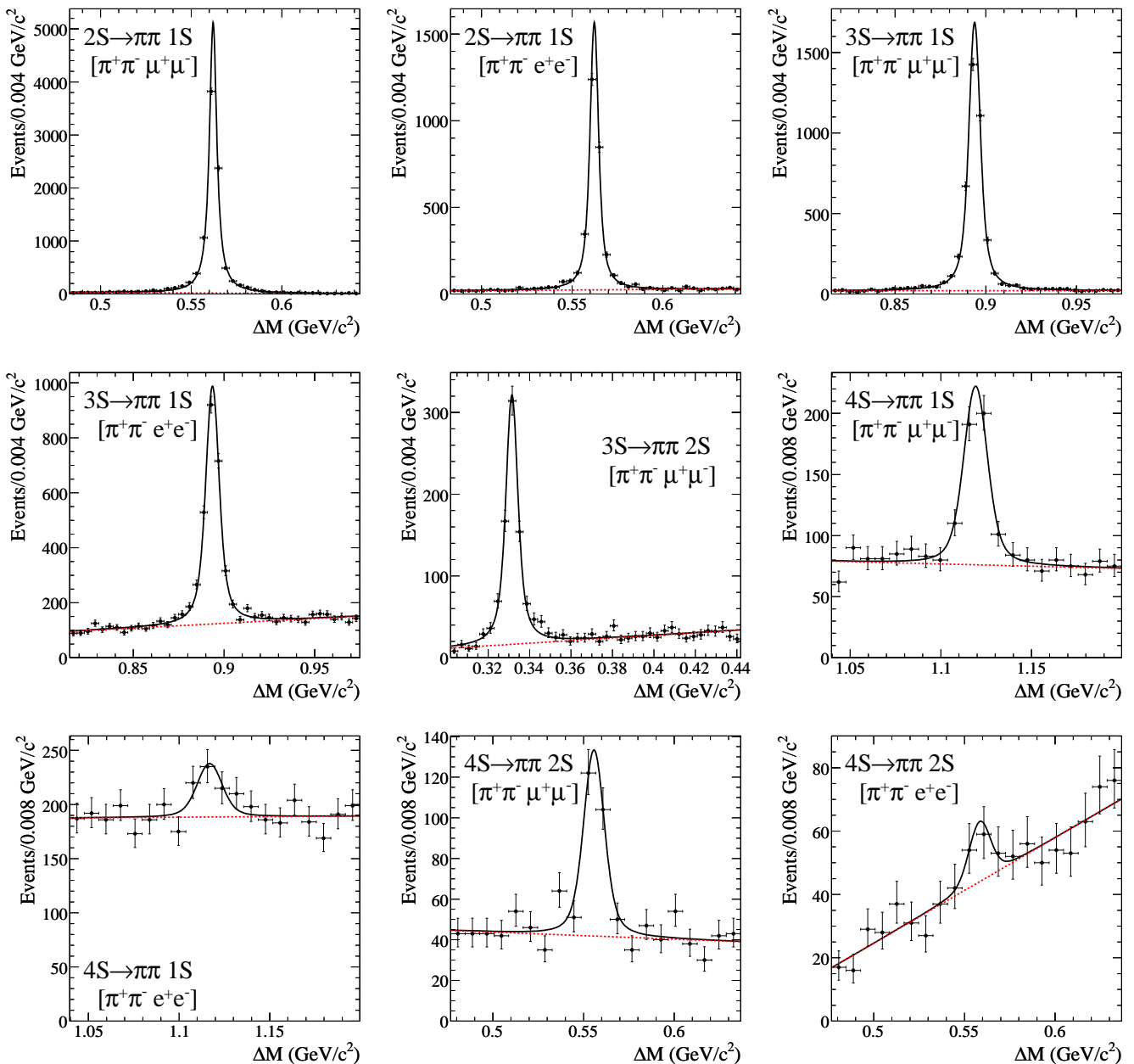


FIG. 2: ΔM distributions of events in the final sample for the $mS \rightarrow \pi\pi nS$ transitions. Data are shown as crosses. The solid lines are the best fit to the data and are only for illustration purposes: they are performed using the signal PDF described in the text with resolution parameters fixed to the values determined on MC events. Dashed lines show the background contribution.

$e^+e^- \rightarrow \eta 1S$ cross section is the same in the “on-peak” and “off-peak” samples by calculating the binomial probability, \mathcal{P} , of observing respectively 56 and 0 events for a binomial coefficient of $p = L_{on}^{int}/(L_{on}^{int} + L_{off}^{int}) = 0.905$, based on the integrated luminosities of the two samples. We obtain $\mathcal{P} = 4 \times 10^{-3}$ and thus we attribute the observed $\eta\Upsilon(1S)$ events to $\Upsilon(4S)$ decays.

The event yields for the $4S \rightarrow \eta 1S$ transition in the ee and $\mu\mu$ final states are determined by unbinned extended maximum likelihood fits to the ΔM_η distribution of the

sample of events in Fig. 3 having $m_{3\pi}$ within 35 MeV/c^2 of the known η mass. The signal PDF is parametrized by a Voigtian function, with resolution parameters fixed to the values determined from MC events, while the background is assumed to be constant. The free parameters in the fits are: ΔM_η^{sig} , the peak position of the signal distribution, N_{sig} and N_{bkg} , the number of signal and background events. The efficiency and acceptance are determined from MC samples. The fits are shown in Fig. 4. The significance, estimated from the likelihood

TABLE II: Results for the products of partial widths and branching fractions for the $\Upsilon(mS)$ hadronic transitions. N_{cand} is the number of candidates in the signal box, N_{bck} is the number of background events from the fit or estimated from data sidebands as described in the text, N_{corr} is the efficiency-corrected number of signal events. The first error is statistical, the second is systematic. All upper limits are 90%CL.

Transition	Our Measurement	N_{cand}	N_{bck}	N_{corr}
$\Gamma_{ee}(2S) \times \mathcal{B}(\Upsilon(2S) \rightarrow \pi^+\pi^-\Upsilon(1S)) \times \mathcal{B}(\Upsilon(1S) \rightarrow \mu^+\mu^-)$	(meV) 2582±28±94	9036	156±11	24319±268
$\Gamma_{ee}(2S) \times \mathcal{B}(\Upsilon(2S) \rightarrow \pi^+\pi^-\Upsilon(1S)) \times \mathcal{B}(\Upsilon(1S) \rightarrow e^+e^-)$	(meV) 2618±60±97	3139	230±9	25202±574
$\Gamma_{ee}(2S) \times \mathcal{B}(\Upsilon(2S) \rightarrow \eta\Upsilon(1S)) \times \mathcal{B}(\Upsilon(1S) \rightarrow \mu^+\mu^-) \times \mathcal{B}(\eta \rightarrow \pi^+\pi^-\pi^0)$	(meV) < 3.1	0	2.5±1.1	< 28
$\Gamma_{ee}(3S) \times \mathcal{B}(\Upsilon(3S) \rightarrow \pi^+\pi^-\Upsilon(1S)) \times \mathcal{B}(\Upsilon(1S) \rightarrow \mu^+\mu^-)$	(meV) 457±8±18	4198	207±10	9945±174
$\Gamma_{ee}(3S) \times \mathcal{B}(\Upsilon(3S) \rightarrow \pi^+\pi^-\Upsilon(1S)) \times \mathcal{B}(\Upsilon(1S) \rightarrow e^+e^-)$	(meV) 441±12±18	3604	1234±20	9821±261
$\Gamma_{ee}(3S) \times \mathcal{B}(\Upsilon(3S) \rightarrow \pi^+\pi^-\Upsilon(2S)) \times \mathcal{B}(\Upsilon(2S) \rightarrow e^+e^-)$	(meV) 206±11±12	975	180±21	4477±241
$\Gamma_{ee}(3S) \times \mathcal{B}(\Upsilon(3S) \rightarrow \eta\Upsilon(1S)) \times \mathcal{B}(\Upsilon(1S) \rightarrow \mu^+\mu^-) \times \mathcal{B}(\eta \rightarrow \pi^+\pi^-\pi^0)$	(meV) < 2.0	1	0.8±0.4	< 41
$\Gamma_{ee}(3S) \times \mathcal{B}(\Upsilon(3S) \rightarrow \eta\Upsilon(1S)) \times \mathcal{B}(\Upsilon(1S) \rightarrow e^+e^-) \times \mathcal{B}(\eta \rightarrow \pi^+\pi^-\pi^0)$	(meV) < 9.6	4	2.8±0.8	< 210
$\mathcal{B}(\Upsilon(4S) \rightarrow \pi^+\pi^-\Upsilon(1S)) \times \mathcal{B}(\Upsilon(1S) \rightarrow \mu^+\mu^-)$	($\times 10^{-6}$) 1.99±0.16±0.07	687	378±11	739±60
$\mathcal{B}(\Upsilon(4S) \rightarrow \pi^+\pi^-\Upsilon(1S)) \times \mathcal{B}(\Upsilon(1S) \rightarrow e^+e^-)$	($\times 10^{-6}$) 1.76±1.05±0.06	1057	934±17	676±397
$\mathcal{B}(\Upsilon(4S) \rightarrow \pi^+\pi^-\Upsilon(2S)) \times \mathcal{B}(\Upsilon(2S) \rightarrow \mu^+\mu^-)$	($\times 10^{-6}$) 1.65±0.21 ±0.11	377	204±8	615±78
$\mathcal{B}(\Upsilon(4S) \rightarrow \pi^+\pi^-\Upsilon(2S)) \times \mathcal{B}(\Upsilon(2S) \rightarrow e^+e^-)$	($\times 10^{-6}$) 1.76±1.03 ±0.11	251	206±8	669±392
$\mathcal{B}(\Upsilon(4S) \rightarrow \eta\Upsilon(1S)) \times \mathcal{B}(\Upsilon(1S) \rightarrow \mu^+\mu^-) \times \mathcal{B}(\eta \rightarrow \pi^+\pi^-\pi^0)$	($\times 10^{-6}$) 1.08±0.17±0.05	40	0.2±0.4	387±60
$\mathcal{B}(\Upsilon(4S) \rightarrow \eta\Upsilon(1S)) \times \mathcal{B}(\Upsilon(1S) \rightarrow e^+e^-) \times \mathcal{B}(\eta \rightarrow \pi^+\pi^-\pi^0)$	($\times 10^{-6}$) 1.15±0.29±0.05	16	0.7±0.6	424±106

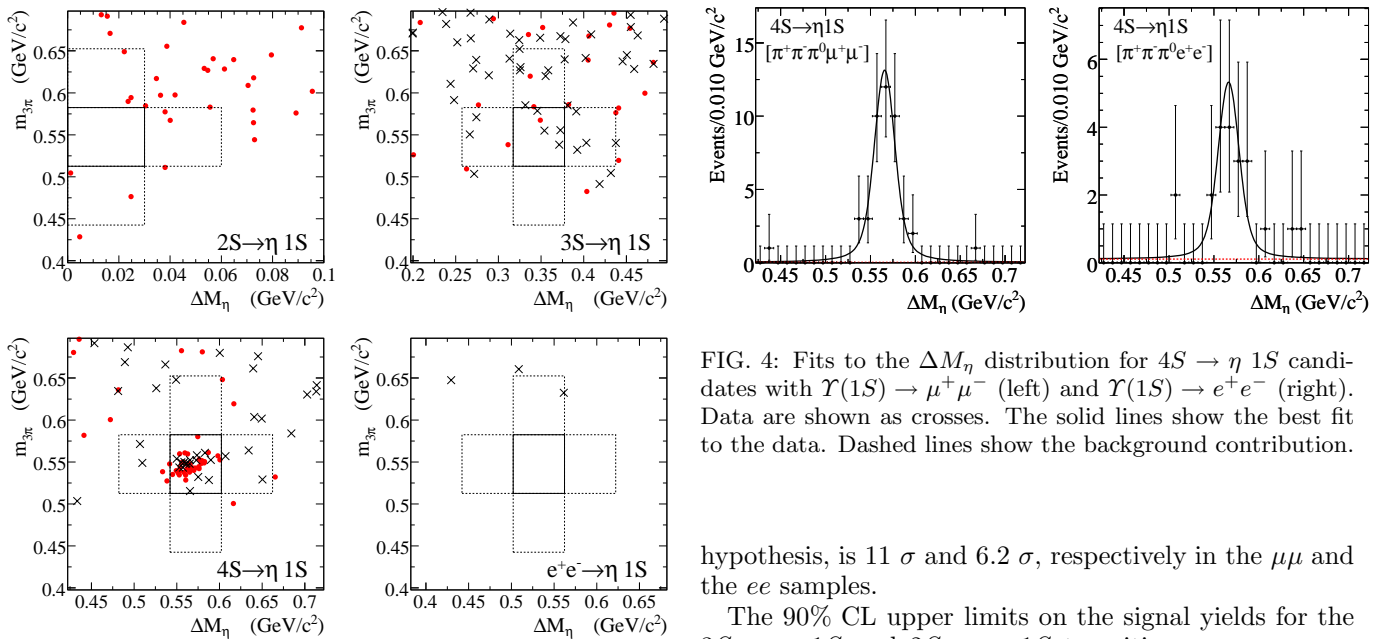


FIG. 3: Distributions of $m_{3\pi}$ vs ΔM_η for the $mS \rightarrow \eta 1S$ transitions studied. Crosses are for the $\Upsilon(1S) \rightarrow e^+e^-$ sample and dots are for the $\Upsilon(1S) \rightarrow \mu^+\mu^-$ sample. Solid lines delimit the signal box region. Dashed lines delimit the sideband regions used for background extrapolation. The signal box for the $2S \rightarrow \eta 1S$ transition (top left) is at the boundary of the kinematically allowed region of ΔM_η and only one sideband can be defined.

ratio $n\sigma \simeq \sqrt{2 \log [\mathcal{L}(N_{sig})/\mathcal{L}(0)]}$ between a fit that includes a signal function and a fit with only a background

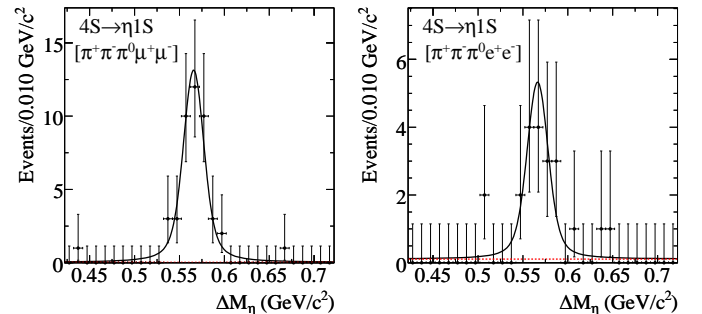


FIG. 4: Fits to the ΔM_η distribution for $4S \rightarrow \eta 1S$ candidates with $\Upsilon(1S) \rightarrow \mu^+\mu^-$ (left) and $\Upsilon(1S) \rightarrow e^+e^-$ (right). Data are shown as crosses. The solid lines show the best fit to the data. Dashed lines show the background contribution.

hypothesis, is 11σ and 6.2σ , respectively in the $\mu\mu$ and the ee samples.

The 90% CL upper limits on the signal yields for the $3S \rightarrow \eta 1S$ and $2S \rightarrow \eta 1S$ transitions are conservatively estimated from the numbers of events in the signal boxes, taking into account the uncertainties in the efficiencies [13]. The background level in the $\mu^+\mu^-$ sample is negligible, and background subtraction in the e^+e^- sample, which also has a lower efficiency, would not affect the result.

V. SYSTEMATIC UNCERTAINTIES

We have considered a number of possible sources of systematic uncertainties, in addition to the number of $\Upsilon(4S)$ [15] and the calculated luminosity for ISR events.

TABLE III: Sources of systematic uncertainties on partial widths or branching fractions and ratios of partial widths, separated into errors that cancel in ratios, errors due to lepton identification (ID) and invariant mass that are common to all transitions, but differ for electrons and muons, and errors that are specific to individual decay modes. All errors are relative and given in percent. We also list the corrections applied to account for differences between data and simulation.

Source	data/MC corr.	$\Upsilon(2S) \rightarrow$		$\Upsilon(3S) \rightarrow$			$\Upsilon(4S) \rightarrow$		
		$\pi\pi\Upsilon(1S)$	$\eta\Upsilon(1S)$	$\pi\pi\Upsilon(1S)$	$\pi\pi\Upsilon(2S)$	$\eta\Upsilon(1S)$	$\pi\pi\Upsilon(1S)$	$\pi\pi\Upsilon(2S)$	$\eta\Upsilon(1S)$
Common systematic errors (cancel in all ratios) (%)									
Number of $\Upsilon(4S)$		–		–			1.1		
ISR luminosity		3.0		3.0			–		
Tracking		1.0		1.0			1.0		
Selection		0.3		0.3			0.3		
p_{cand}^* cut		0.3		0.3			0.3		
Systematic errors associated to lepton identification or invariant mass (%)									
Muon ID	1.025	0.6		0.6			0.6		
$M(\mu^+\mu^-)$ cut	1.006	0.2		0.2			0.2		
Electron ID	1.011	0.7		0.7			0.7		
$M(e^+e^-)$ cut	0.998	0.5		0.5			0.5		
Systematic errors specific to each mode (%)									
π^0 efficiency	1.033	–	3.6	–	–	3.6	–	–	3.6
Acceptance		0.3	–	1.7	4.7	–	2.6	6.0	–
Fitting		1.6	1.6	1.6	1.6	1.6	1.6	1.6	1.6
Total e^+e^- (%)		3.7	–	4.1	–	5.1	3.5	6.5	4.4
Total $\mu^+\mu^-$ (%)		3.7	5.1	4.0	5.9	5.1	3.5	6.5	4.3
Total on ratios (%)		–	4.3	–	5.5	4.6	–	6.9	5.0

The uncertainties in charged track and π^0 reconstruction efficiencies are determined by a comparison of data and MC events on independent control samples. The systematic uncertainties associated with the event selection, the cut on p_{cand}^* , the $M_{\ell\ell}$ invariant mass cut, and the lepton identification criteria are estimated by comparing the efficiencies determined from MC samples to the corresponding efficiencies measured with the ISR $mS \rightarrow \pi\pi nS$ samples in the modes where there are sufficiently high statistics and low background to allow the comparison. The efficiencies are determined from the numbers of signal events which pass or fail any given cut, after all other cuts are applied.

The systematic uncertainties due to the choice of signal and background parameterizations are estimated by using different functions or different parameters, and by varying the ΔM or ΔM_η fit ranges. The uncertainty in the acceptance correction for the $mS \rightarrow \pi\pi nS$ transitions is determined by the change in the signal yields when using different $m_{\pi\pi}$ and $\cos\theta_h$ binnings.

The systematic uncertainties from all these sources are summarized in Table III for each transition. The total systematic uncertainty is estimated by adding in quadrature all different contributions. We apply correction factors to the efficiency determined from MC events, accounting for differences between data and MC samples in the π^0 reconstruction, in lepton identification, and in the $M_{\ell\ell}$ cut.

VI. RESULTS

The products of branching fractions and partial widths for each transition are given Table II. They are determined from the efficiency-corrected yield in each mode, after correcting for small differences between data and MC samples and taking into account the number of $\Upsilon(4S)$ or the equivalent ISR luminosity, \mathcal{K} . For a narrow vector resonance produced in ISR

$$\mathcal{K} = L_{on}^{int} \frac{12\pi^2}{M(mS)s} W\left(s, 1 - \frac{M^2(mS)}{s}\right) \quad (2)$$

where the QED “radiator” function $W(s, x)$ is calculated to second order following [16–18].

Averaging the results from the e^+e^- and the $\mu^+\mu^-$ final states, taking into account the common systematic errors, and using the world average values of $\mathcal{B}(\eta \rightarrow \pi^+\pi^-\pi^0)$ and $\mathcal{B}(\Upsilon(nS) \rightarrow \ell^+\ell^-)$ [12] we obtain the partial widths and ratios of partial widths listed in Table IV. In this Table, we also compare our results to the values expected for each quantity based on previous measurements of $\Upsilon(mS)$ widths and branching fractions. The measured values of the $\Upsilon(2S)$ and $\Upsilon(3S)$ total widths are used to derive the theoretical expectations for branching fractions from the predicted partial widths in [2].

The values of $\mathcal{B}(\Upsilon(4S) \rightarrow \pi^+\pi^-\Upsilon(1S)) \times \mathcal{B}(\Upsilon(1S) \rightarrow \mu^+\mu^-)$ and $\mathcal{B}(\Upsilon(4S) \rightarrow \pi^+\pi^-\Upsilon(2S)) \times \mathcal{B}(\Upsilon(2S) \rightarrow \mu^+\mu^-)$ supersede our previously reported values based

TABLE IV: Our measurements for the products and ratios of partial widths and branching fractions of $\Upsilon(mS)$ hadronic transitions, with comparisons to previous measurements and theoretical expectations. We also report the values of the branching fractions that are derived from our measurements using world average values for $\Gamma_{ee}(nS)$. All upper limits are 90% CL. The values of the last seven branching fractions in this Table (reported below the horizontal line) are not independent from the values reported above. The values of $\mathcal{B}(\Upsilon(4S) \rightarrow \pi^+\pi^-\Upsilon(nS))$ from Ref. [12] and indicated with an asterisk are based on our previous measurement [3] performed on a subset of the current sample. As discussed in the text, part of the difference in the central values is ascribed to a more accurate estimate of the acceptance.

		This work	PDG [12]	Prediction
$\Gamma_{ee}(2S) \times \mathcal{B}(\Upsilon(2S) \rightarrow \pi^+\pi^-\Upsilon(1S))$	(eV)	$105.4 \pm 1.0 \pm 4.2$	115 ± 5	
$\Gamma(\Upsilon(2S) \rightarrow \eta\Upsilon(1S))/\Gamma(\Upsilon(2S) \rightarrow \pi^+\pi^-\Upsilon(1S))$	($\times 10^{-3}$)	< 5.2	< 11	2.5 [2]
$\Gamma_{ee}(3S) \times \mathcal{B}(\Upsilon(3S) \rightarrow \pi^+\pi^-\Upsilon(1S))$	(eV)	$18.46 \pm 0.27 \pm 0.77$	19.8 ± 1.0	
$\Gamma(\Upsilon(3S) \rightarrow \pi^+\pi^-\Upsilon(2S))/\Gamma(\Upsilon(3S) \rightarrow \pi^+\pi^-\Upsilon(1S))$		$0.577 \pm 0.026 \pm 0.060$	0.63 ± 0.14	0.3 [2]
$\Gamma(\Upsilon(3S) \rightarrow \eta\Upsilon(1S))/\Gamma(\Upsilon(3S) \rightarrow \pi^+\pi^-\Upsilon(1S))$	($\times 10^{-2}$)	< 1.9	< 5	1.7 [2]
$\mathcal{B}(\Upsilon(4S) \rightarrow \pi^+\pi^-\Upsilon(1S))$	($\times 10^{-4}$)	$0.800 \pm 0.064 \pm 0.027$	$0.90 \pm 0.15^{(*)}$	–
$\Gamma(\Upsilon(4S) \rightarrow \pi^+\pi^-\Upsilon(2S))/\Gamma(\Upsilon(4S) \rightarrow \pi^+\pi^-\Upsilon(1S))$		$1.16 \pm 0.16 \pm 0.14$		–
$\Gamma(\Upsilon(4S) \rightarrow \eta\Upsilon(1S))/\Gamma(\Upsilon(4S) \rightarrow \pi^+\pi^-\Upsilon(1S))$		$2.41 \pm 0.40 \pm 0.12$	–	–
<hr/>				
$\mathcal{B}(\Upsilon(2S) \rightarrow \pi^+\pi^-\Upsilon(1S))$	(%)	$17.22 \pm 0.17 \pm 0.75$	18.8 ± 0.6	27 ± 2 [2]
$\mathcal{B}(\Upsilon(2S) \rightarrow \eta\Upsilon(1S))$	($\times 10^{-4}$)	< 9	< 20	8.1 ± 0.8 [14]
$\mathcal{B}(\Upsilon(3S) \rightarrow \pi^+\pi^-\Upsilon(1S))$	(%)	$4.17 \pm 0.06 \pm 0.19$	4.48 ± 0.21	3.3 ± 0.3 [2]
$\mathcal{B}(\Upsilon(3S) \rightarrow \pi^+\pi^-\Upsilon(2S))$	(%)	$2.40 \pm 0.10 \pm 0.26$	2.8 ± 0.6	1.0 ± 0.1 [2]
$\mathcal{B}(\Upsilon(3S) \rightarrow \eta\Upsilon(1S))$	($\times 10^{-4}$)	< 8	< 22	6.7 ± 0.7 [14]
$\mathcal{B}(\Upsilon(4S) \rightarrow \pi^+\pi^-\Upsilon(2S))$	($\times 10^{-4}$)	$0.86 \pm 0.11 \pm 0.07$	$0.88 \pm 0.19^{(*)}$	–
$\mathcal{B}(\Upsilon(4S) \rightarrow \eta\Upsilon(1S))$	($\times 10^{-4}$)	$1.96 \pm 0.06 \pm 0.09$	–	–

on a fraction of the current sample [3]. Part of the difference in the central values is due to the different methods used to determine the acceptance, which was calculated in our previous paper assuming a phase-space distribution in the $\Upsilon(4S) \rightarrow \pi^+\pi^-\Upsilon(nS)$ decay. The efficiency is not uniform over the Dalitz plot, thus the impact on the central value between the two methods depends on the angular distributions peculiar of each transition. The difference can be estimated by comparing the value of the phase-space averaged efficiencies ε_{PS} , and the effective efficiencies ε_{eff} calculated from the observed event yields in each region of the Dalitz plot

$$\varepsilon_{eff} = \frac{\sum_{i=1}^{nbins} N_{sig}^i}{\sum_{i=1}^{nbins} N_{sig}^i / \varepsilon_i}. \quad (3)$$

Notice that the uncertainty in the calculated effective efficiency is due to the statistical uncertainty in the event yield. As shown in Table I the effective efficiency for $\Upsilon(4S) \rightarrow \pi^+\pi^-\Upsilon(1S)$, when the $\Upsilon(1S)$ decays to $\mu^+\mu^-$, is $\sim 7\%$ larger than the value estimated using a phase-space distribution. Accounting for this difference, the results presented here are statistically compatible with the ones previously reported.

From our result we derive new values for $\mathcal{B}(\Upsilon(3S, 2S) \rightarrow \pi^+\pi^-\Upsilon(1S))$ that are of comparable precision to the previous world averages, and compatible with them. The value of $\mathcal{B}(\Upsilon(3S) \rightarrow \pi^+\pi^-\Upsilon(2S))$ derived from our measurement has an error that is smaller than the current world average.

VII. CONCLUSIONS

We have presented a study of hadronic transitions between the Υ states: new measurements of the branching fractions $\mathcal{B}(\Upsilon(4S) \rightarrow \pi^+\pi^-\Upsilon(1S, 2S))$, $\mathcal{B}(\Upsilon(3S) \rightarrow \pi^+\pi^-\Upsilon(2S))$ which have smaller errors than current world averages, and new measurements of $\mathcal{B}(\Upsilon(3S, 2S) \rightarrow \pi^+\pi^-\Upsilon(1S))$ whose precision is comparable to present world averages. We have also presented measurements of the ratios of partial widths $\Gamma(\Upsilon(mS) \rightarrow \pi^+\pi^-\Upsilon(2S))/\Gamma(\Upsilon(mS) \rightarrow \pi^+\pi^-\Upsilon(1S))$ ($m = 3, 4$) where a number of systematic uncertainties cancel. Our results for the branching fractions of the $\Upsilon(2S)$ and $\Upsilon(3S) \rightarrow \eta\Upsilon(1S)$ transitions represent improvements over the current published upper limits, and are compatible with the recent results from CLEO [8]: $\mathcal{B}(\Upsilon(2S) \rightarrow \eta\Upsilon(1S)) = (2.1_{-0.6}^{+0.7} \pm 0.5) \times 10^{-4}$, $\mathcal{B}(\Upsilon(3S) \rightarrow \eta\Upsilon(1S)) < 2.9 \times 10^{-4}$ at 90% CL.

We observe a significant number of $\eta\Upsilon(1S)$ candidates at the formation energy of the $\Upsilon(4S)$. We can exclude the hypothesis that they are due to continuum $e^+e^- \rightarrow \eta\Upsilon(1S)$ with a probability of 99.6% and we attribute them to $\Upsilon(4S)$ decays. The branching fraction for the $\Upsilon(4S) \rightarrow \eta\Upsilon(1S)$ decay is larger than the branching fraction for $\Upsilon(4S) \rightarrow \pi^+\pi^-\Upsilon(1S)$, which is unexpected when compared to all other known charmonium and bottomonium transitions. There are no predictions for this specific decay mode. In the QCEDME calculation for hadronic transitions, the effect of the nodes in the wave functions in the overlap integrals be-

tween the initial and final states and the intermediate states can be large for radial excitations. But even that should not significantly affect the ratio of partial widths $\Gamma(\Upsilon(4S) \rightarrow \eta\Upsilon(1S))/\Gamma(\Upsilon(4S) \rightarrow \pi^+\pi^-\Upsilon(1S))$, at least if the $\Upsilon(4S) \rightarrow \eta\Upsilon(1S)$ transition is E1M2 [2]. It is possible that accidental cancellations suppress the E1M2 term with respect to M1M1, or perhaps QCDME becomes unreliable for higher gluon momenta. These results, together with the recent CLEO measurement of the matrix elements in $\Upsilon(3S) \rightarrow \pi^+\pi^-\Upsilon(1S, 2S)$ and $\Upsilon(2S) \rightarrow \pi^+\pi^-\Upsilon(1S)$ transitions [19], could provide a tool to understand the hadronic transitions better.

VIII. ACKNOWLEDGMENTS

We are grateful for the extraordinary contributions of our PEP-II colleagues in achieving the excellent luminosity and machine conditions that have made this work possible. The success of this project also relies critically on

the expertise and dedication of the computing organizations that support *BABAR*. The collaborating institutions wish to thank SLAC for its support and the kind hospitality extended to them. This work is supported by the US Department of Energy and National Science Foundation, the Natural Sciences and Engineering Research Council (Canada), the Commissariat à l'Énergie Atomique and Institut National de Physique Nucléaire et de Physique des Particules (France), the Bundesministerium für Bildung und Forschung and Deutsche Forschungsgemeinschaft (Germany), the Istituto Nazionale di Fisica Nucleare (Italy), the Foundation for Fundamental Research on Matter (The Netherlands), the Research Council of Norway, the Ministry of Education and Science of the Russian Federation, Ministerio de Educación y Ciencia (Spain), and the Science and Technology Facilities Council (United Kingdom). Individuals have received support from the Marie-Curie IEF program (European Union) and the A. P. Sloan Foundation.

-
- [1] For a recent review on heavy quarkonia, see N. Brambilla *et al.* [Quarkonium Working Group], arXiv:hep-ph/0412158.
 - [2] Y. P. Kuang, *Front. Phys. China* **1**, 19 (2006) and references therein.
 - [3] B. Aubert *et al.* [*BABAR* Collaboration], *Phys. Rev. Lett.* **96**, 232001 (2006).
 - [4] A. Sokolov *et al.* [*Belle* Collaboration], *Phys. Rev. D* **75**, 071103 (2007).
 - [5] F. Butler *et al.* [*CLEO* Collaboration], *Phys. Rev. D* **49**, 40 (1994).
 - [6] P. Moxhay, *Phys. Rev. D* **39**, 3497 (1989); H. Y. Zhou and Y. P. Kuang, *Phys. Rev. D* **44**, 756 (1991); F. K. Guo, P. N. Shen, H. C. Chiang and R. G. Ping, *Nucl. Phys. A* **761**, 269 (2005); V. V. Anisovich, D. V. Bugg, A. V. Sarantsev and B. S. Zou, *Phys. Rev. D* **51**, 4619 (1995); M. Uehara, *Prog. Theor. Phys.* **109**, 265 (2003); H. W. Ke, J. Tang, X. Q. Hao and X. Q. Li, *Phys. Rev. D* **76**, 074035 (2007).
 - [7] In the rest of the paper $m = 4, 3, 2$ and $n = 2, 1$ unless specified otherwise.
 - [8] Q. He *et al.* [*CLEO* Collaboration], arXiv:0806.3027 [hep-ex].
 - [9] B. Aubert *et al.* [*BABAR* Collaboration], *Nucl. Instrum. Meth. Phys. Res., Sect. A* **479**, 1 (2002).
 - [10] D. J. Lange, *Nucl. Instrum. Meth. Phys. Res., Sect. A* **462**, 152 (2001).
 - [11] S. Agostinelli *et al.*, *Nucl. Instrum. Meth. Phys. Res., Sect. A* **506**, 250 (2003).
 - [12] W. M. Yao *et al.* [Particle Data Group], *J. Phys. G* **33** (2006) 1 and 2007 partial update for the 2008 edition available on the PDG WWW pages <http://pdg.lbl.gov/>
 - [13] R. Barlow, *Comput. Phys. Commun.* **149**, 97 (2002).
 - [14] E. Eichten, S. Godfrey, H. Mahlke and J. L. Rosner, arXiv:hep-ph/0701208.
 - [15] B. Aubert *et al.* [*BABAR* Collaboration], *Phys. Rev. D* **67**, 032002 (2003) [arXiv:hep-ex/0207097].
 - [16] M. Benayoun, S. I. Eidelman, V. N. Ivanchenko and Z. K. Silagadze, *Mod. Phys. Lett. A* **14**, 2605 (1999).
 - [17] G. Bonneau and F. Martin, *Nucl. Phys. B* **27**, 381 (1971).
 - [18] V. N. Baier, V. S. Fadin and V. A. Khoze, *Nucl. Phys. B* **65**, 381 (1973).
 - [19] D. Cronin-Hennessy *et al.*, [*CLEO* Collaboration] *Phys. Rev. D* **76**, 072001 (2007).